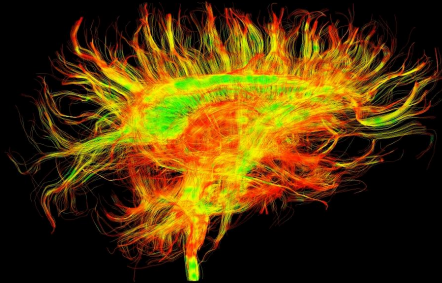# Computational Diffusion MRI : Models, Algorithms and Applications

Rachid DERICHE

Odyssée Project Team

INRIA Sophia Antipolis - Méditerranée Research Center

National and Kapodistrian University of Athens - 10/24/2008

INRIA

Eight Research Centers

# Computational Neurosciences
Measuring, Modeling and simulating

▶ Single and assemblies of neurons, Cortical columns and areas

▶ The human brain anatomical connectivity

▶ The functioning of the human brain through its electrical activity

and some of its Applications

  ▶ Clinical Brain Research

  ▶ Brain Computer Interface

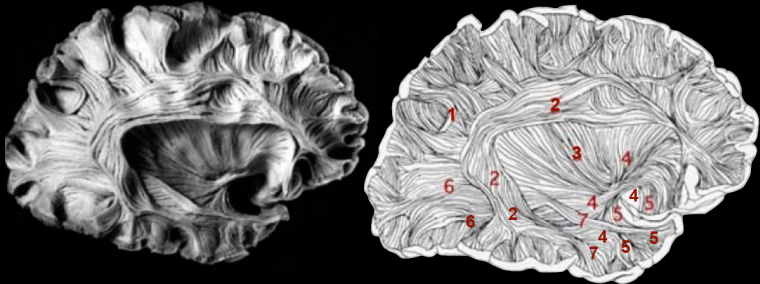 ▶ Computational and biological vision.
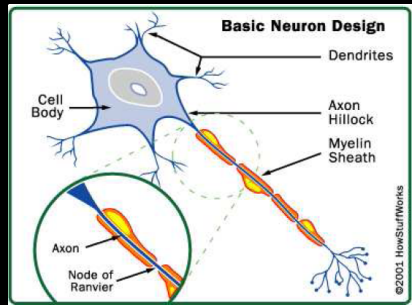
Anatomy of Cerebral White Matter (I)
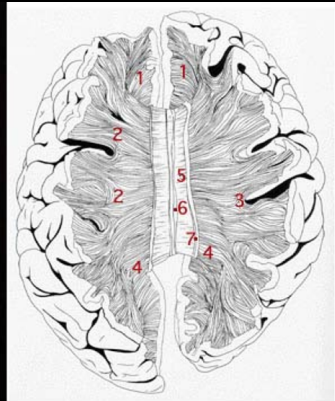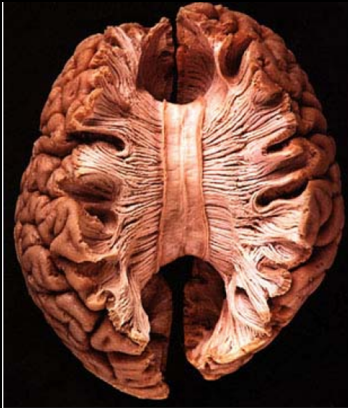
1. Frontal forceps 2. Corpus callosum commissural fibers 3. Short arcuate fibers 4. Occipital forceps 5. Indusium griseum 6. Medial longitudinal stria 7. Lateral longitudinal stria

Corpus Callosum and its radiation (images from [Williams-etal:97])

Anatomy of Cerebral White Matter (II)

Images from [Williams-etal97]

1. Short arcuate bundles, **2.** Superior longitudinal fasciculus, **3.** External capsule, **4.** Inferior occipitofrontal fasciculus, **5.** Uncinate fasciculus, **6.** Sagittal stratum, **7.** Inferior longitudinal fasciculus

Short and Long Association tracts in the right hemisphere (images from [Williams-etal:97])

Corticostriate Pathway: From all parts of the cerebral cortex to the striatum

WM Fiber Structures of the Human Brain

Corpus callosum

ponto-cerebellar tracts

pyramidal fiber pathways

fornix

uncinate fasciculus

superior longitudinal fasciculus

inferior longitudinal fasciculus
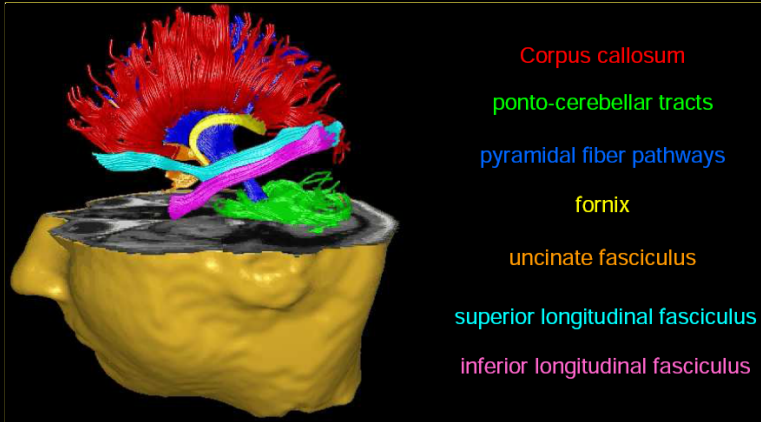
WM Fibers structures : Image from [A.Leemans-PhD:06]

Diffusion MRI

- ▶ MRI introduced by **Paul C. Lauterbur** and **Peter Mansfield** in **1973**, jointly Nobel Prize in Physiology/Medicine - 2003.

- ▶ DMRI is a recent imaging modality that measures, **in vivo and non-invasively**, the random motion of water molecules in biological tissues

- ▶ The random motion of water molecules reflects the **structure and the architecture** of the biological tissues

- ▶ Pioneering and related contributions discussed by **Denis Le Bihan** (cras:85,ismrm:85), **Moseley** (bmr:84), **Merboldt** (mjmr:85)...

Diffusion Tensor MRI and beyond...

▶ Water Diffusion is anisotropic : Formalism of **Diffusion Tensor** (DT-MRI) introduced by **Peter Basser** in 1994 to correct the scalar model (Basser-Mattiello-LeBihan:94,J Magn Reson B)

▶ Important invariant quantities can be extracted (Eigenvalues, Trace, Det, FA..)

▶ High Angular Resolution Diffusion Imaging (DSI, Q-Ball, tuch-mrm:2002)

From Images to WM Fibers through DMRI

▶ **Estimation and Regularization**
Diffusion Tensors from noisy DWI Images
(tschumperle-deriche:pami:2005;lenglet-deriche:jmiv:06)

▶ **Connectivity**
How to recover the geometric description of the anatomical
connectivity between brain areas ?
(descoteaux-deriche:tmi:08)

▶ **Segmentation**
How to recover a set of coherently oriented white matter
fibers population? (lenglet-deriche:tmi:2006;jmiv:06,
wassermann-deriche:biomed:08)

▶ **Q-Ball Imaging**
How to deal with HARDI data and Fibers Crossings
(descoteaux-deriche:mrm:06;mrm:07;jmiv:08)

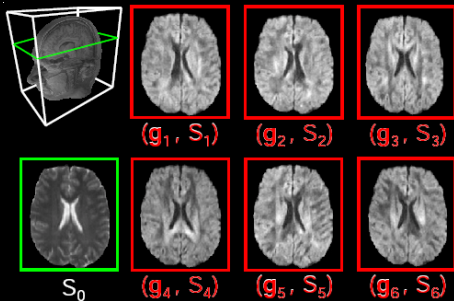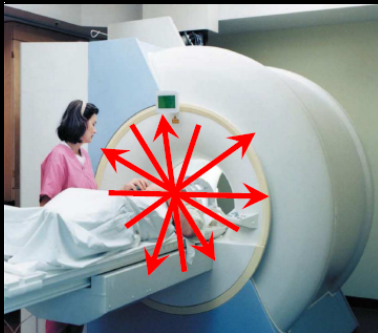# Diffusion MRI : Basic Principles I

▶ Diffusion can be measured using a magnetic field B_0, two RF and gradient pulses that magnetically label moving water molecules

▶ The scanner applies first a **constant magnetic field B_0** over the sample tissue

▶ The spins of the **water molecule align** along B_0 and causes a **net magnetization** of the sample

A MRI Scanner
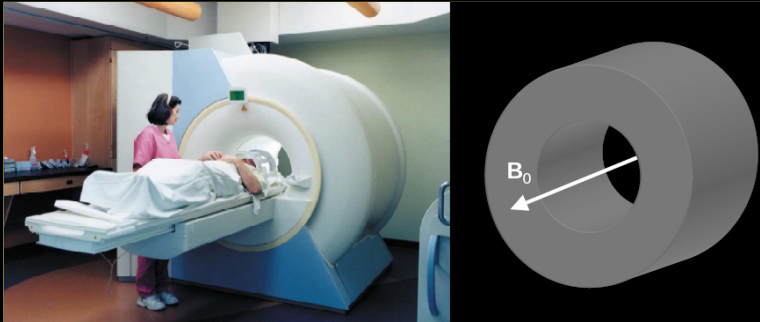
The scanner applies a constant magnetic field $\mathbf{B_0}$

Diffusion MRI Image Formation

Acquisition of several raw images under different magnetic fields.

Diffusion MRI : Basic Principles II

▶ **A 90 degree RF pulse** followed after a time **Δ** with **a 180 degrees RF pulse** with a gradient strength G induces **a phase shift** proportional to the spin displacement :
$\delta(\phi) = \gamma \delta \mathbf{G}.(\mathbf{r} - \mathbf{r_0})$

▶ The total magnetization encodes the displacement for moving spins
$\frac{S}{S_0} = \int_{-\infty}^{+\infty} e^{i\gamma\delta\mathbf{G}.(\mathbf{r}-\mathbf{r_0})} P(\mathbf{r} \mid \mathbf{r_0}, \delta) d\mathbf{r} d\mathbf{r_0}$

▶ For **free diffusion** in an homogeneous domain, there is a **close form distribution**

DT-MRI Image Formation (I)

▶ **For free diffusion in an homogeneous domain,** the probability to find a spin initially at $\mathbf{r_0}$ at position $\mathbf{r}$ after a time interval Δ is :

$$P(\mathbf{r} \mid \mathbf{r_0}, \Delta) = \frac{1}{\sqrt{(4\pi\Delta)(det(\mathbf{D}))}} e^{-(\frac{(\mathbf{r}-\mathbf{r_0})^t \mathbf{D}^{-1}(\mathbf{r}-\mathbf{r_0})}{4\Delta})}$$

▶ Combining the equations, we obtain :

$$\frac{S}{S_0} = e^{-\gamma^2 \delta^2 (\Delta - \delta/3) \mathbf{G}^t \mathbf{D} \mathbf{G}}$$

▶ With $\mathbf{G} = \mid G \mid \mathbf{g}$ and $b = (\gamma \mid G \mid \delta)^2 (\Delta - \frac{\delta}{3})$
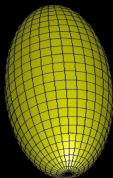
$$\frac{S}{S_0} = e^{-b \mathbf{g}^t \mathbf{D} \mathbf{g}}$$
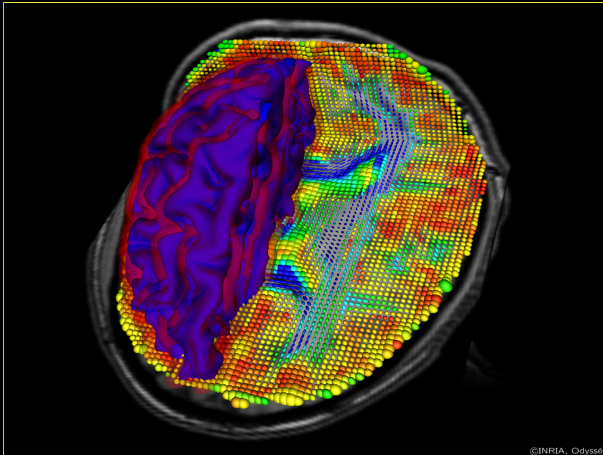
DT-MRI Image Formation (II)

▶ Diffusion described by $\mathbf{D}_{(x,y,z)}$, an SPD $3*3$ matrix, which explains through the **Stejskal-Tanner equation** the measurements S_k obtained :

$$\forall (x, y, z), \qquad S_{k_{(x,y,z)}} = S_{0_{(x,y,z)}} \, e^{-b g_k^T \mathbf{D}_{(x,y,z)} g_k}$$

▶ The **diffusion Tensors** can be visualized as **ellipsoids** :
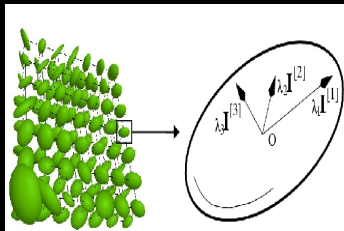
DT-MRI Processing

Diffusion tensors estimated from CMRR data

DT-MRI Images : Direct estimation of the tensors

▶ Direct estimation (Westin etal:02) :

$$\mathbf{D} = \sum_{k=1}^{6} -\frac{1}{b} \ln\left(\frac{S_k}{S_0}\right) \, g_k g_k^T$$

▶ [⊕] S_0 and at least six non-colinear diffusion gradient directions, i.e 7 images are then theoretically sufficient.

▶ [⊖] Results are very sensitive to noise.

▶ [⊖] Positive definiteness of the tensors is not insured.

DT-MRI Images : Least square estimation

- When $n > 7$ raw images are available, **D** can be retrieved by a least square method :

$$\min_{\mathbf{D}} \sum_{k=1}^{n} \left(-\frac{1}{b} \ln \left(\frac{S_k}{S_0} \right) - g_k^T \mathbf{D} g_k \right)^2 \quad \Rightarrow \quad \left\{ \begin{array}{l} AX = b \\ \hat{X} = (A^T A)^{-1} A^T b \end{array} \right.$$

- [⊕] Least square methods are more robust to noise, by using all the raw image informations.

- [⊖] Positive definiteness of the tensors is not insured.

- **Reprojection of the tensors is needed for both estimation methods.**

Variational approaches for tensor estimation & regularization

▶ **Estimation**

Minimize the criterion, in the constrained tensor space :

$$\min_{\mathbf{D} \in \mathrm{P}(3)} \int_{\Omega} \sum_{k=1}^{n} \psi \left(\left| \ln \left(\frac{S_0}{S_k} \right) - g_k^T \mathbf{D} g_k \right| \right) + \alpha \; \phi(\|\nabla \mathbf{D}\|) \; d\Omega$$

▶ **Regularization**

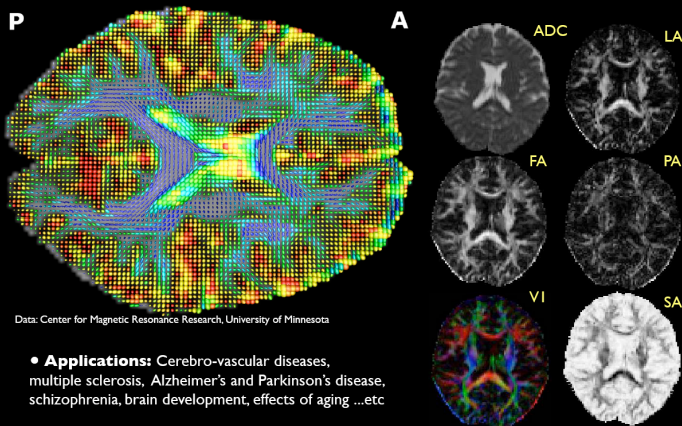Minimize the following regularisation functional f, as :

$$\min_{X \in ConstrainedSpace} f(X) = \int_{\Omega} \phi(\|\nabla_{\Omega} X\|) + \frac{\alpha}{2}(X - X_0)^2 \; d\Omega$$

The Corpus Callosum regularized
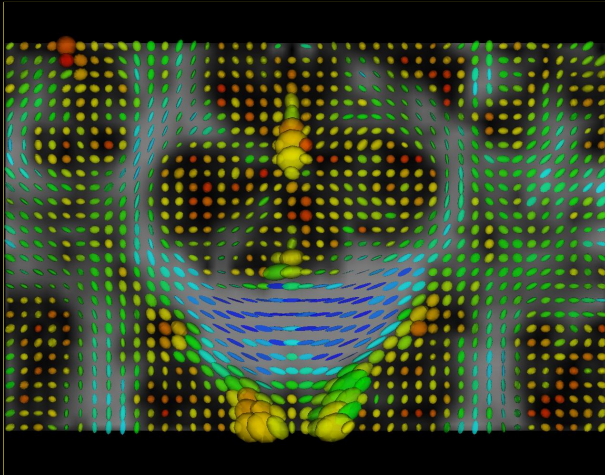
Characterizing Tissue Microstructure

- $FA = \frac{\sqrt{3((\lambda_1 - \lambda_2)^2 + (\lambda_2 - \lambda_3)^2 + (\lambda_3 - \lambda_1)^2)}}{\sqrt{2(\lambda_1^2 + \lambda_2^2 + \lambda_3^2)}}; \; VR = \frac{\lambda_1 \lambda_2 \lambda_3}{\bar{\lambda}}$

- $c_l = \frac{\lambda_1 - \lambda_2}{3\bar{\lambda}}; \; c_p = 2\frac{\lambda_2 - \lambda_3}{3\bar{\lambda}}; \; c_s = \frac{\lambda_3}{\bar{\lambda}}$


P   A

Data: Center for Magnetic Resonance Research, University of Minnesota

ADC   LA

FA   PA

VI   SA

- **Applications:** Cerebro-vascular diseases, multiple sclerosis, Alzheimer's and Parkinson's disease, schizophrenia, brain development, effects of aging ...etc

Towards Anatomical Connectivity Mapping

▶ The water diffusion in many regions of the white matter is highly anisotropic

▶ The orientation of the principale eigenvector $u(.)$ of $\mathbf{D}$ represents the predominant axonal direction of white matter fiber, represented by a 3D curve $c(t)$

Streamlines Propagation

Classical streamlines estimation expected to coincide with neural paths
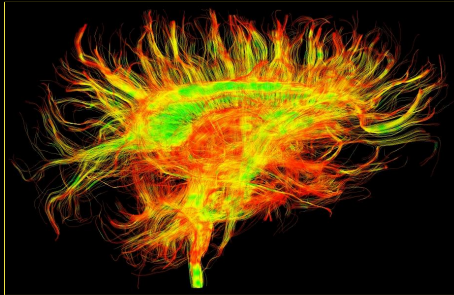
Whole brain tractography [8000 fibers / 5 min]
Euler, Runge-Kutta integration scheme with DTI interpolation

Fibers as geodesics in the white matter

▶ **Use the entire tensor information** and see the White matter as a surface with a metric given by $\mathbf{D}^{-1}$

▶ We can compute a distance function ϕ in the intrinsic white matter as :

$$|\nabla \phi|^2 = \frac{\partial \phi}{\partial x_i} \frac{\partial \phi}{\partial x_j} g^{ij} = 1, \qquad (1)$$

▶ **Fibers** can be extracted individually **as geodesics** in ϕ

Tractography: Real Dataset

Top 10% connections to the CC splenium
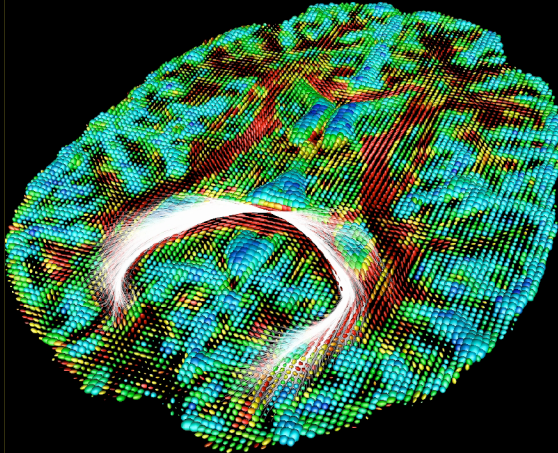
Data: CMRR, University of Minnesota

Geodesic distance:
[Jackowski-etal05]: 7 min
[Lenglet-etal04]: 20 min

Geodesics:
About 3 min / 15,000 fibers

Our FM Algorithm:
7 seconds

Data: 128x128x60
PC: 1.7 GHz / 1.5 Gb RAM

Diffusion Tensor MRI Segmentation

▶ Given a DT-MRI volumic image I

▶ Evolve an initial surface S to segment I using all the information provided by the Diffusion tensor..
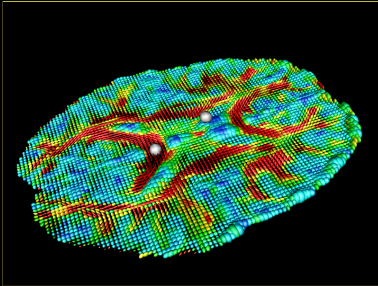
Corpus-Callosum
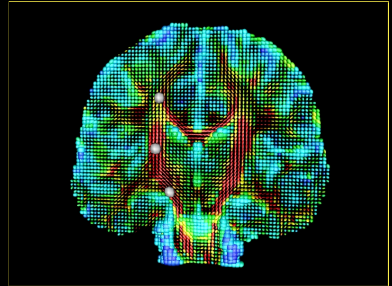
Cortico-Spinal Tract

Level-set based segmentation using the GAR framework
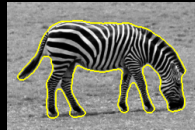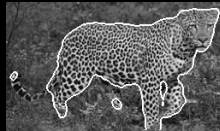
Scalar   Color   Texture   Color + Texture

DTI Segmentation and Surface Evolution (I)

▶ Use the Kullback-Liebler divergence to measure the distance between Gaussian distributions and induce a distance between Diffusion tensors [Wang-Vemuri:04]

▶ Tensor distance as the square root of the J-divergence, a symmetrized version of the KL Divergence:

$$d(\mathbf{T}_1, \mathbf{T}_2) = \frac{1}{2}\sqrt{tr(\mathbf{T}_1^{-1}\mathbf{T}_2 + \mathbf{T}_2^{-1}\mathbf{T}_1) - 2n}$$

▶ Closed form expression for the mean μ of a set of T

   ▶ Euclidean 0 and Euclidean 1 and Euclidean 2

   ▶ Euclidean 0 and J-Divergence 1 and J-Divergence 2

DTI Segmentation and Surface Evolution (II)

▶ The geodesic distance between any two fixed mean and m-variate normal distributions Σ_1 and Σ_2 wis shown to be :

$$\mathcal{D}(\Sigma_1, \Sigma_2) = \sqrt{\frac{1}{2}\text{tr}(\log^2(\Sigma_1^{-1/2}\Sigma_2\Sigma_1^{-1/2}))} = \sqrt{\frac{1}{2}\sum_{i=1}^{m}\log^2(\eta_i)}$$

where η_i denote the m eigenvalues of the matrix $\Sigma_1^{-1/2}\Sigma_2\Sigma_1^{-1/2} \in S^+$.

▶ **Properties of $\mathcal{D}$:** $\mathcal{D}$ is indeed a distance on S^+ and exhibits nice properties.

▶ Geodesic 1 and Geodesic 2

On DTI Distance, Gradient, Mean and beyond...

Euclidean	J-divergence	Geodesic
$\mathrm{tr}\left((A-B)(A-B)^T\right)$	$\frac{1}{4}\left(\mathrm{tr}\left(A^{-1}B+B^{-1}A\right)-6\right)$	$\frac{1}{2}\mathrm{tr}\left(\log^2\left(A^{-1/2}BA^{-1/2}\right)\right)$
$A-B$	$\frac{1}{4}(B^{-1}-A^{-1}BA^{-1})$	$A\log\left(B^{-1}A\right)$
$\frac{1}{N}\sum_{i=1}^{N}\Sigma_i$	$V^{-1/2}\left(U^{1/2}VU^{1/2}\right)^{1/2}V^{-1/2}$ with $U=\frac{1}{N}\sum_{i=1}^{N}\Sigma_i$ and $V=\frac{1}{N}\sum_{i=1}^{N}\Sigma_i^{-1}$	Algorithm

Lenglet/Rousson/Deriche "Statistics on the Manifold of Multivariate Normal Distributions: Theory and Application to Diffusion Tensor MRI Processing", Journal of Mathematical Imaging and Vision, 2006
Lenglet/Rousson/Deriche "DTI Segmentation by Statistical Surface Evolution", IEEE Transactions on Medical Imaging, 2006

R. Deriche

Algorithm for Mean of tensors

Algorithm 1 Riemannian estimation of the mean diffusion tensor

Require: $\{\Sigma_i\} \in S^+(3), i = 1, \ldots N$ and nit, the number of iterations

Ensure: $\overline{\Sigma}_g$, the mean tensor

1: $M \leftarrow \mathscr{I}$
2: **for** $k = 1$ to nit **do**
3:    $V \leftarrow \mathbb{O}$ $\{3 \times 3$ zero matrix$\}$
4:    **for** $i = 1$ to N **do**
5:      $V \leftarrow \log(\Sigma_i^{-1} M)$
6:    **end for**
7:    $V = (1/N)MV$
8:    $M \leftarrow M^{1/2}\exp(-M^{-1/2}VM^{-1/2})M^{1/2}$
9: **end for**
10: Return M

Further results : On the Geodesic

▶ The geodesic starting from $\Sigma(t_1) \in S^+$ in the direction $\dot{\Sigma}(t_1) = \Sigma(t_1)^{1/2} X \Sigma(t_1)^{1/2}$ with $\dot{\Sigma}(t_1), X \in S = TS^+$ is given by:

$$\Sigma(t) = \Sigma(t_1)^{1/2} \exp(tX) \Sigma(t_1)^{1/2} \in S^+, \forall t \in [t_1, t_2]$$
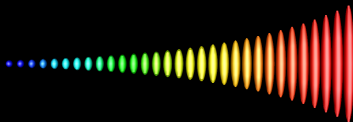
(a): Geodesic Interpolation   (b) : Euclidean Interpolation
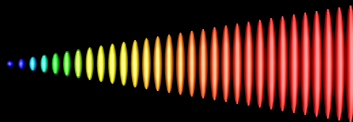
DTI Segmentation on Real Data

▶ Segmentation of the corpus callosum in real DTI:
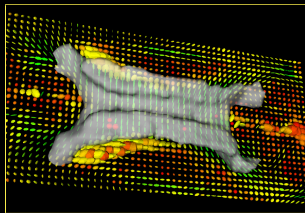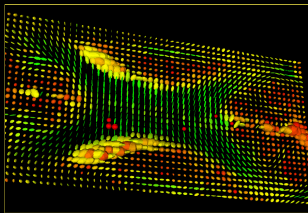
Euclidean Distance

J-Divergence
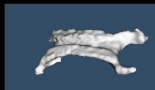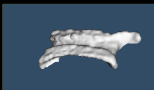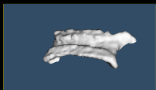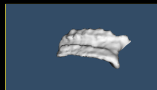
Geodesic Distance

Limitations of DTI
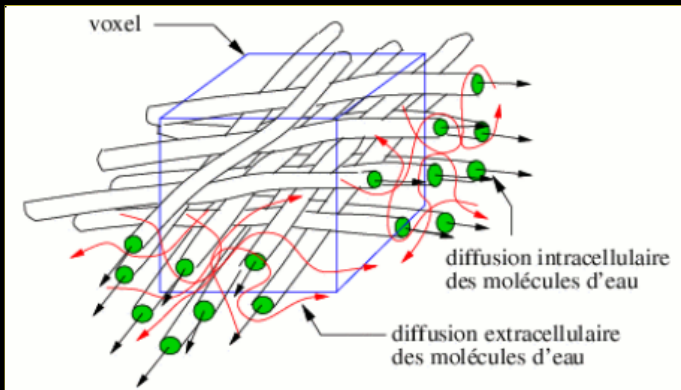
DTI fails when fiber bundles crosses within the same voxel

Non-Gaussian diffusion process - Image from [Poupon-PhD:99]

HARDI : High Angular Resolution Diffusion Imaging
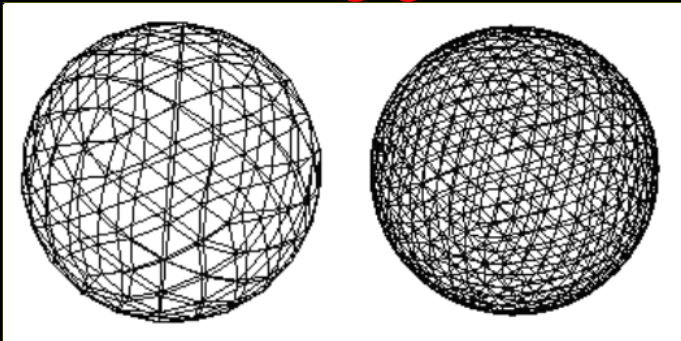
- ▶ Use of N gradient directions : 162, 252 ..
- ▶ Process all discrete noisy data on the sphere using SH

$$S(\Theta_i, \Phi_i) = \sum_{j=1}^{R} c_j Y_j(\Theta_i, \Phi_i) \quad or \quad \mathbf{S} = \mathbf{BC}$$

Solving for SH Coefficients

- Classical LS : Minimize $(\mathbf{S} - \mathbf{BC})^t(\mathbf{S} - \mathbf{BC})$
- Smooth solution on the sphere : Laplace-Beltrami regularization
- Minimize $E(\mathbf{S}) = \int_\sigma (\Delta_b \mathbf{S})^2 d\sigma$
- SH obey the PDE : $\Delta_b \mathbf{S} + l(l+1)\mathbf{S} = 0$

Solving for SH Coefficients

▶ New criterion :

$$E(\mathbf{S}) = (\mathbf{S} - \mathbf{BC})^t(\mathbf{S} - \mathbf{BC}) + \lambda \mathbf{C}^t \mathbf{LC}$$

▶ $\mathbf{L}$ is the $R \times R$ matrix with entries $\ell_j^2(\ell_j + 1)^2$ along the diagonal (ℓ_j is the order associated with the jth coefficient).

▶ Closed form solution :

$$\mathbf{C} = (\mathbf{B}^t\mathbf{B} + \lambda \mathbf{L})^{-1}\mathbf{B}^t\mathbf{S}$$

▶ Smooth solution on the sphere with a penalty for higher order term.

Attenuation and Diffusion MRI Signal

The attenuation of the MRI signal is given by : $S(g) = S_0 exp(-bD(g))$

Diffusion MRI signal : S(g)
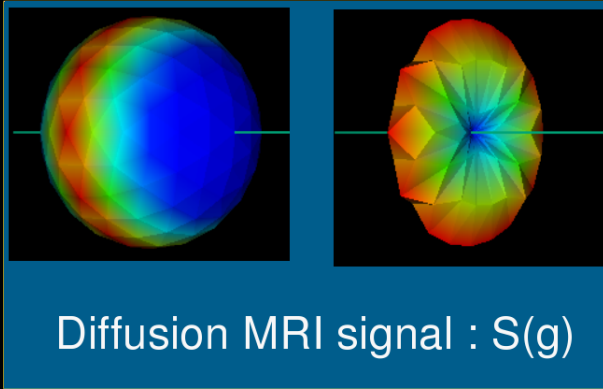
Red : not attenuated - Blue : highly attenuated

Q-Ball Imaging
ODF can be computed directly from HARDI

$$\Psi(\mathbf{u}) = \int_0^\infty P(\alpha.\mathbf{u})d\alpha$$

[Tuch; MRM04]
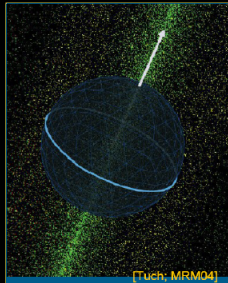
Integral over the perpendicular equator = Funk Radon Transform

$$G[f(\mathbf{w})](\mathbf{u}) = \int \delta(\mathbf{u}^t\mathbf{w})f(\mathbf{w})d\mathbf{w} \equiv \text{ODF}$$

Analytical ODF
ODF can be computed analytically from SH coefficients

$$\Psi(\mathbf{u}) = \sum_{j=1}^{R} 2\pi P_{\ell_j}(0) c_j Y_j(\mathbf{u}).$$

where $P_\ell(0)$ the Legendre polynomial of degree ℓ evaluated at 0,

$$P_\ell(0) = \begin{cases} 0 & \ell \text{ odd} \\ (-1)^{\ell/2} \dfrac{1 \cdot 3 \cdot 5 \cdots (\ell-1)}{2 \cdot 4 \cdot 6 \cdots \ell} & \ell \text{ even} \end{cases}$$

Fast speed-up factor of 15 with classical QBI

Validated against ground truth and classical QBI

Funck Radon Transform (I)

1 fiber
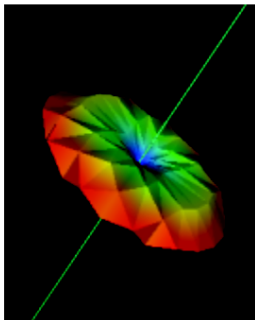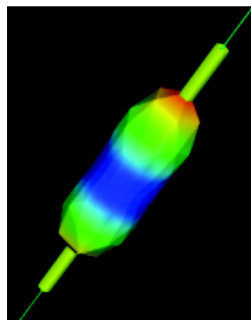
Signal S → FRT[S]

FRT is the line integral along the equator plane

Funck Radon Transform (II)

2 fibers

Signal S → FRT[S]
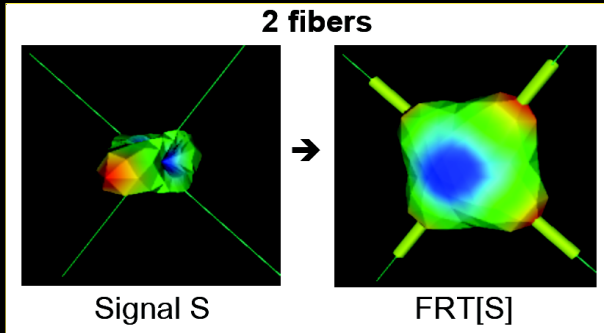
FRT allows to effectively recover the fibers direction

ODF and FRT allows to effectively recover the fibers direction

1. **A**pparent **D**iffusion **C**oefficient (**ADC**)
2. **O**rientation **D**istribution **F**unction (**ODF**)

Fiber distribution
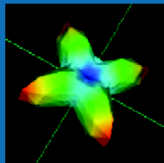
ADC profile
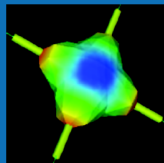
Diffusion **ODF**

Descoteaux, Deriche et al in "Magnetic Resonance in Medicine", 2007

Biological phantom
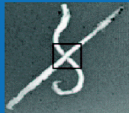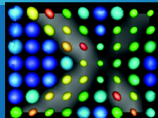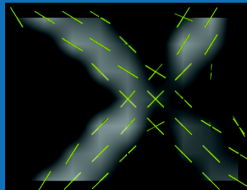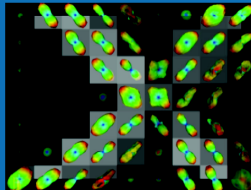
Rat Biological Phantom - Data from McGill - BIC

Real Data : Crossing between the CC, CST and SLF..)

q-ball ODFs

diffusion tensors
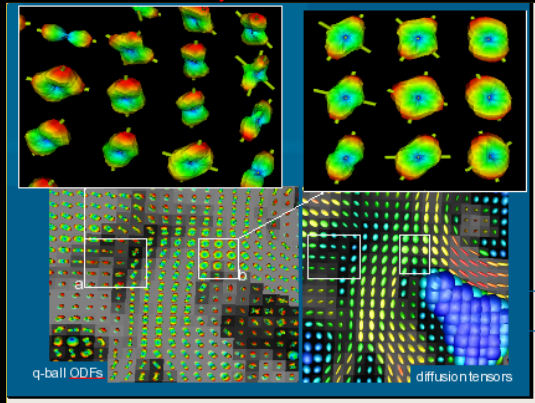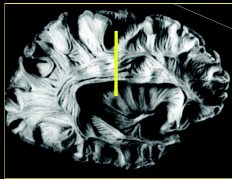
HARDI : Reconstruction and Processing

HARDI Signal

QBI
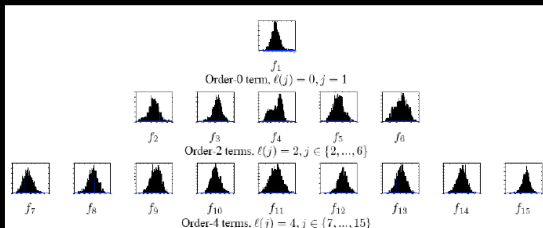
HARDI segmentation

Deconvolution

Fiber tractography
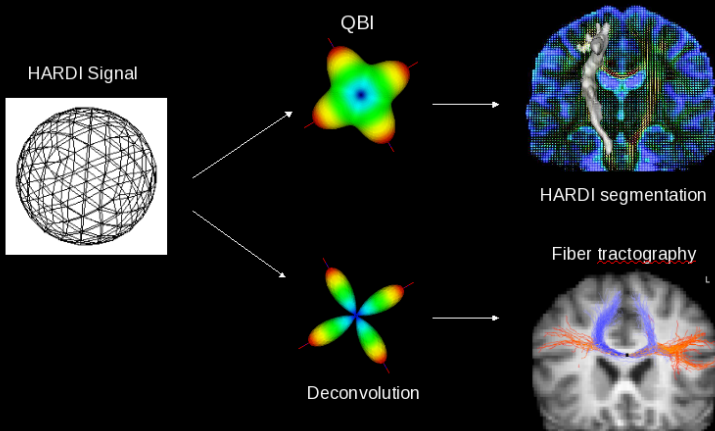
Descoteaux/Deriche : IEEE TMI:2008, JMIV:2008

ODF Segmentation based on SH (I)

- Dissimilarity measure: L2 norm of SH coefficients difference

$$\langle \psi, \psi' \rangle = \int_{S^2} \psi(r).\psi'(r)dr = \int_{S^2} \left(\sum_{i=1}^{R} c_i Y_i(r) \right) \left(\sum_{i=1}^{R} c_i' Y_i(r) \right) dr = \sum_{i=1}^{R} c_i.c_i'$$

$$\Rightarrow \|\psi - \psi'\|^2 = \sum_{i=1}^{R} (c_i - c_i')^2$$
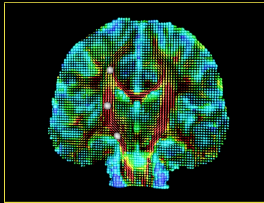
- Assumption of Gaussian distribution for SH coefficients:

f_1

Order-0 term, $\ell(j) = 0, j = 1$

f_2　f_3　f_4　f_5　f_6

Order-2 terms, $\ell(j) = 2, j \in \{2, ..., 6\}$

f_7　f_8　f_9　f_{10}　f_{11}　f_{12}　f_{13}　f_{14}　f_{15}

Order-4 terms, $\ell(j) = 4, j \in \{7, ..., 15\}$

Distribution in manual segmentation of Corpus Callosum

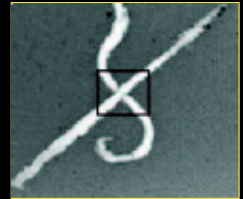[Descoteaux-etal JMIV 2008]

ODF Segmentation based on SH (II)
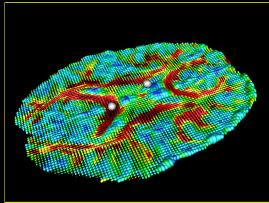
Corpus-Callosum   Cortico-Spinal Tract   Biol. Phantom

Descoteaux/Deriche " HARDI MRI Segmentation Using Region-Based Statistical Surface Evolution". Journal of Mathematical Imaging in Vision, in press 2008

Deterministic vs Probabilistic Tractography

- Efficient
- Vulnerable to initialization
- Vulnerable to principal direction
- Output: streamlines

- Slower
- Robust to initialization
- Accounts for uncertainty in principal direction
- Output: quantitative connectivity map
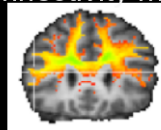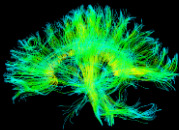
Descoteaux, Deriche et al "IEEE Transactions in Medical Imaging", 2008. In press.
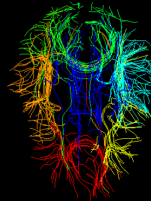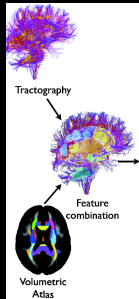
Extracting ODF Maxima as Stationary Points of Constrained Homogeneous Polynomial
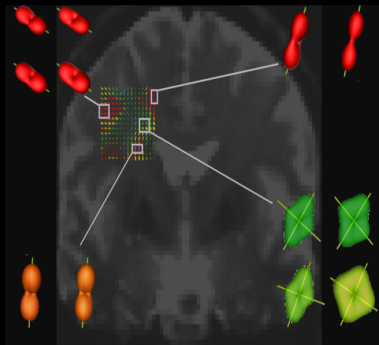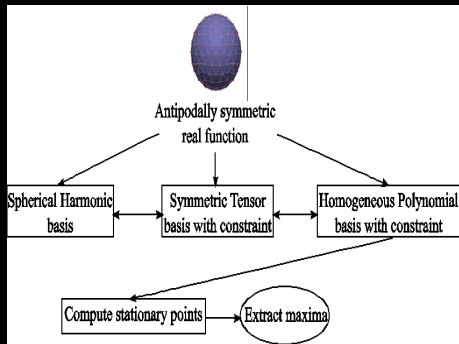
Workshop MICCAI-CDMRI, Sept. 10, 2008 (with A.Ghosh, E. Tsigaridas etal)

White Matter Fibers Clustering

▶ **Data** Given a set of tensors, fibers, define a distance and an affinity matrix

▶ **Embedding :** N-Cuts, Laplacian EigenMaps, Diffusion Maps.

▶ **Clustering :** K Means..

Wassermann/Descoteaux/Deriche."Diffusion Maps Clustering for MR Q-Ball Imaging Segmentation." International Journal on Biomedical Imaging, 2008.

R. Deriche

Application : Detection of multiple pathways in the spinal cord using q-ball imaging

- ▶ Application to an ex vivo spinal cord of one cat using a 3T scanner, 100 directions and b-values varying from 1000 to 3000 s/mm2.

- ▶ QBI can retrieve crossing fibre information, where the diffusion tensor imaging approach is constrained to a single diffusion direction.

- ▶ First study demonstrating the benefits of QBI in observing longitudinal, commissural and dorso-ventral fibres in the spinal cord.

- ▶ First step towards in vivo characterization of the healthy and injured spinal cord using HARDI/Q-Ball
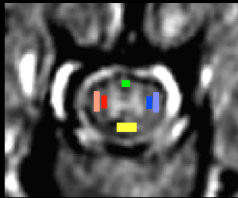
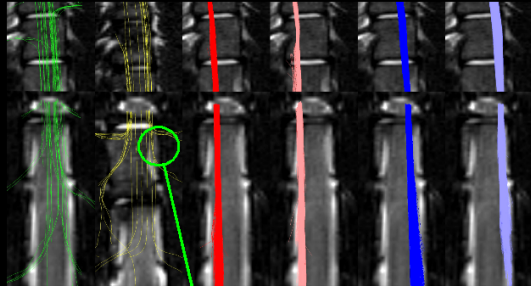# DW-MRI of Spinal Cord Injury
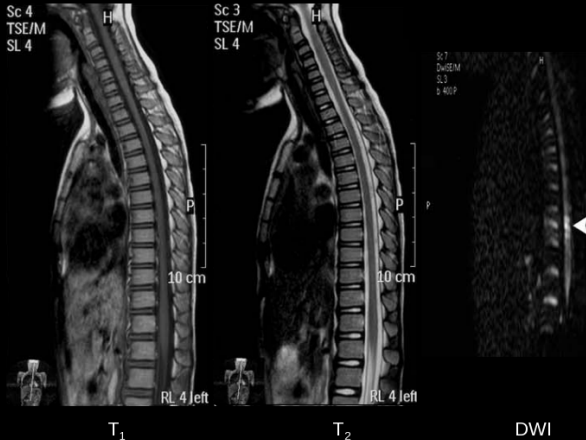
T₁ — $\rightarrow$ No abnormality

T₂ — $\rightarrow$ No abnormality

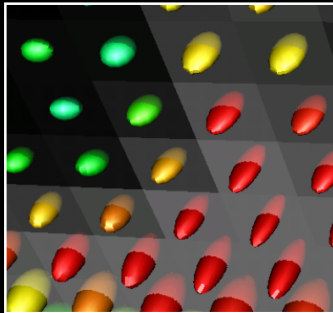DWI — $\rightarrow$ Hypersignal

Tractography of the Cat Spinal Cord

Tractography
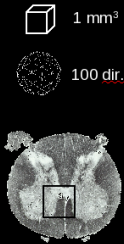
Crossing fibers that are not taken into account using the tensor model
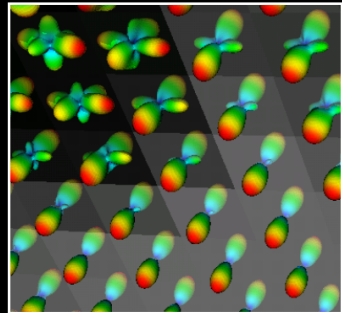→ *Need for a less constraining approach*

Q-Ball Imaging of the Spinal Cord (I)

1 mm³

100 dir.

DTI   Q-Ball

Cohen-Adad,Descoteaux et al, Neuroimage, 42, 739-749, 2008

Q-Ball Imaging of the Spinal Cord (II)
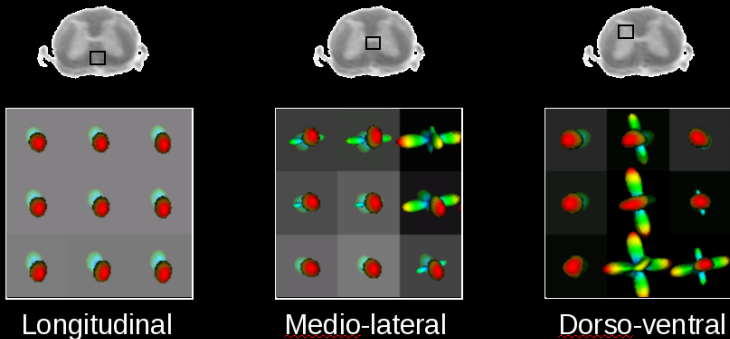

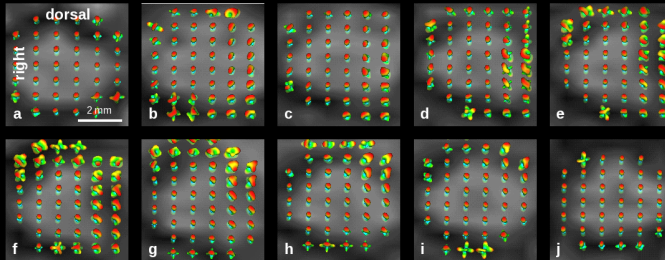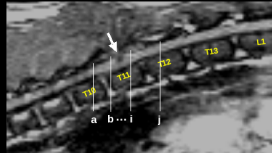Longitudinal   Medio-lateral   Dorso-ventral

Cohen-Adad,Descoteaux et al, Neuroimage, 42, 739-749, 2008

Q-Ball Imaging of the Spinal Cord (III)

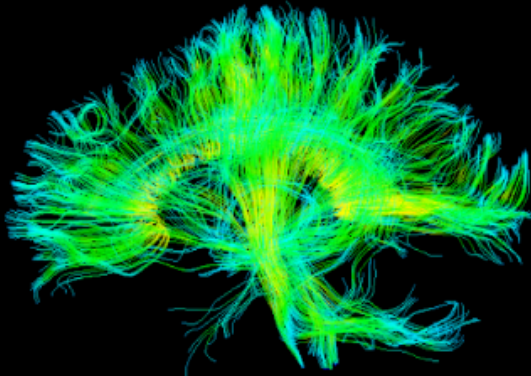Cohen-Adad,Descoteaux et al, Neuroimage, 42, 739-749, 2008

Collaborations/Acknowledgments

- U678 INSERM, CHU Pitié-Salpêtrière (H. Benali) et CHUPS/CENIR Centre de NeuroImagerie de Recherche (S. Lehericy)
- CEA - SHFJ / NeuroSpin (C.Poupon/Mangin) - La Timone - Marseille (J.L.Anton)
- MPI - Leipzig (PAI Procore) (A.Anwander/ T.Knosche)
- CMRR - Minneapolis (NSF/INRIA) (K. Ugurbil,G. Sapiro)
- McGill - BIC - Montreal (INRIA/FQRNT) (J. Campbell/B. Pike/K. Siddiqi)
- NIH - NICHD - Bethesda (P.Basser/C.Pierpaoli/E.Ozarslan)
- Some algorithms are plugins of the BrainVisa Software package (SHFJ-IFR 49) and Slicer3D.
- The INRIA Odyssée Geodesic Connectivity Mapping Library $http : //gcm.gforge.inria.fr/index.html$

Recent Publications/Acknowledgments

- Lenglet/Rousson/Deriche/ "DTI Segmentation by Statistical Surface Evolution", **IEEE Transactions on Medical Imaging, 2006**
- Lenglet/Rousson/Deriche/Faugeras "Statistics on the Manifold of Multivariate Normal Distributions: Theory and Application to Diffusion Tensor MRI Processing", **Journal of Mathematical Imaging and Vision, 2006**
- Descoteaux/Angelino/Fitzgibbons/Deriche "ADC from HARDI: Estimation and Applications", **Magnetic Resonance in Medicine, 2006**
- Descoteaux/Angelino/Fitzgibbons/Deriche "Regularized, Fast, and Robust Analytical Q-Ball Imaging", **Magnetic Resonance in Medicine, 2007**
- Descoteaux/Deriche/Knosche/Anwander "Deterministic and Probabilistic Tractography Based on Complex Fiber Orientation Distributions" **IEEE Transactions in Medical Imaging, 2008. In press.**
- Wassermann/Descoteaux/Deriche."Diffusion Maps Clustering for Magnetic Resonance Q-Ball Imaging Segmentation." **International Journal on Biomedical Imaging, 2008.**
- Related work on Fibers Clustering with D.Wassermann and on High Order Tensors with A.Ghosh **Miccai:08 and Workshops on Sept. 10th**
- Other related papers : $http : //www - sop.inria.fr/odyssee/en/rachid.deriche$

ευχαριστω!

ερωτησεις?